Development/Plasticity/Repair

TrkB Downregulation Is Required for Dendrite Retraction in Developing Neurons of Chicken Nucleus Magnocellularis

Leslayann C. Schecterson,[1] Jason Tait Sanchez,[2] Edwin W. Rubel,[2,3] and Mark Bothwell[1]

[1]Institute for Stem Cell and Regenerative Medicine and Department of Physiology and Biophysics, University of Washington, Seattle, Washington 98109, [2]The Virginia Merrill Bloedel Hearing Research Center, Department of Otolaryngology, Head, and Neck Surgery, University of Washington, Seattle, Washington 98195, and [3]Department of Physiology and Biophysics, University of Washington, Seattle, Washington 98195

The chick embryo (*Gallus domesticus*) is one of the most important model systems in vertebrate developmental biology. The development and function of its auditory brainstem circuitry is exceptionally well studied. These circuits represent an excellent system for genetic manipulation to investigate mechanisms controlling neural circuit formation, synaptogenesis, neuronal polarity, and dendritic arborization. The present study investigates the auditory nucleus, nucleus magnocellularis (NM). The neurotrophin receptor TrkB regulates dendritic structure in CNS neurons. TrkB is expressed in NM neurons at E7–E8 when these neurons have dendritic arbors. Downregulation of TrkB occurs after E8 followed by retraction of dendrites and by E18 most NM cells are adendritic. Is cessation of TrkB expression in NM necessary for dendritic retraction? To answer this question we combined focal *in ovo* electroporation with transposon mediated gene transfer to obtain stable expression of Doxycycline (Dox) regulated transgenes, specifically TrkB coexpressed with EGFP in a temporally controlled manner. Electroporation was performed at E2 and Dox added onto the chorioallointoic membrane from E7.5 to E16. Expression of EGFP had no effect on development of the embryo, or cell morphology and organization of auditory brainstem nuclei. NM cells expressing EGFP and TrkB at E17–E18 had dendrites and biophysical properties uncharacteristic for normal NM cells, indicating that cessation of TrkB expression is essential for dendrite retraction and functional maturation of these neurons. These studies indicate that expression of transposon based plasmids is an effective method to genetically manipulate events in mid to late embryonic brain development in chick.

Introduction

The chick auditory system has been extensively studied for over three decades because its neural circuitry is similar to mammalian auditory neural circuitry and is more accessible for experimental manipulation. The timing of important events such as developmental cell death, axon targeting, dendritogenesis, and synaptogenesis is thoroughly described, providing a firm foundation for studies examining the mechanisms that control these events (Rubel and Parks, 1988, Rubel and Fritzsch, 2002). However, the only widely used method for genetic manipulation of chick embryos employs electroporation of plasmid encoded genes at embryonic day 2 (E2), which typically achieves only transient expression. This is problematic as this transient expression typically ceases before dendritogenesis, and synaptogenesis in hindbrain neurons commences after E9.

Received May 10, 2012; revised Aug. 14, 2012; accepted Aug. 15, 2012.

Author contributions: L.C.S., J.T.S., E.W.R., and M.B. designed research; L.C.S. and J.T.S. performed research; L.C.S. and J.T.S. analyzed data; L.C.S., J.T.S., E.W.R., and M.B. wrote the paper.

This work was supported by NIH Grants R21 DC011504 (M.B.) and R01 DC003829 (E.W.R.). We thank Glen MacDonald for assistance with digital imaging, Frances Lefcort for providing a plasmid encoding chicken TrkB, Xiaozhong Wang for providing Piggybac-based plasmids, and Yoshiko Takahashi and Nicolas Daudet for providing tol2-based plasmids.

The authors declare no competing financial interests.

Correspondence should be addressed to Dr. Mark Bothwell, Department of Physiology and Biophysics, Institute for Stem Cell and Regenerative Medicine, UW Medicine South Lake Union, University of Washington, Box 358056, Seattle, WA 98109-8056. E-mail: mab@uw.edu.

DOI:10.1523/JNEUROSCI.2274-12.2012

 0270-6474/12/3214000-10$15.00/0

Recent studies describe stable expression of genes introduced into chick embryos using vector systems based on *Tol2* and *PiggyBac* (PB) transposons (Sato et al., 2007, Lu et al., 2009). Temporal control was achieved by placing gene expression under control of tetracycline or tamoxifen-related drugs. The present study adapts these vector systems to study mechanisms regulating the development of auditory circuits that process binaural low-frequency information to achieve sound localization and segmentation. Nucleus magnocellularis (NM) and nucleus laminaris (NL), the avian analogs of human ventral cochlear nucleus and medial superior olive (MSO), are key elements of this circuit. Remarkably, chickens represent a more useful model of function of the equivalent human circuits than genetically tractable rodents such as mice because MSO is poorly developed in mice, which lack low-frequency hearing.

Excitatory input from the periphery travels via neurons of the cochlear ganglion (CG; VIIIth nerve), which synapse on NM in the brainstem. Axons from NM neurons bifurcate; one branch projects to the dorsal dendrites and soma of ipsilateral NL neurons and the other branch crosses the midline to synapse on the ventral dendrites and soma of the contralateral NL. Embryonic NM neurons transiently develop dendritic arbors at E7–E8 as they migrate into position in the brainstem. In-growing axonal terminals from CG neurons synapse onto these dendrites. However, NM neurons retract their dendrites, beginning at E11. The extent of retraction varies along the rostrocaudal axis of the nucleus, with caudal-most neurons retaining a substantial dendritic

arbor. As dendrites retract, CG axonal terminals remodel to enwrap the cell soma in calycal terminals known as endbulbs of Held (Jhaveri and Morest, 1982a,b). These calycal terminals provide the sole excitatory input to NM neurons in the mature circuit (Parks, 1981).

The neurotrophin receptor TrkB promotes dendritic growth and synaptogenesis in several neuronal populations (Xu et al., 2000, Yacoubian and Lo, 2000, Luikart et al., 2005). Previous studies indicated that NM neurons express TrkB at E7–E8, but not thereafter (Cochran et al., 1999). The cessation of TrkB expression by NM neurons preceding their retraction of dendrites suggested the hypothesis that downregulation of TrkB is responsible for dendritic retraction. We have tested this hypothesis using doxycycline (Dox)-regulated expression of TrkB encoded by a *Tol2* transposable element vector to prolong TrkB expression in NM neurons at times beyond E8.

Materials and Methods

Plasmids. The *Tol2* constructs pT2K-CAGGS-rtTA-M2, pT2K-BI-TRE-EGFP, pT2K-CAGGS-DsRed, and transposase pCAGGS-T2TP were obtained from Yoshiko Takahashi (Nara Institute of Science and Technology, Nara, Japan) (Sato et al., 2007). pT2K-CAGGS-mbEGFP was constructed by Nicolas Daudet (Vertebrate Development Laboratory, Cancer Research UK, London, UK.) by inserting the coding sequence for membrane-associated EGFP into pT2K-CAGGS obtained from Y. Takahashi. A plasmid containing the coding region of chick TrkB was obtained from Francis Lefcort (University of Montana, Bozeman, MT). The coding region was amplified by PCR, creating a 5′NheI site and 3′ EcoRV site for cloning into pT2K-BI-TRE-EGFP using in-fusion HD cloning (Clontech). The *PiggyBac* plasmids pCAGGS-PBase and pPB-CAG-loxP-DsRed-loxP-EGFP were obtained from Xiaozhong Wang (Northwestern University, Evanston, IL). Plasmids were prepared for *in ovo* electroporation using Qiagen Hi Speed maxi prep (Clontech), precipitated, and concentrated in sterile dH20.

In ovo *electroporation.* All studies used embryos of either sex. Fertilized eggs of white leghorn chickens (*Gallus domesticus*; Featherland Farms) were incubated at 37°C in a tabletop egg incubator (Lyon Technologies). At ~48–50 h or Hamilton–Hamburger (HH) stage 12, eggs were removed for electroporation. *In ovo* electroporation was performed as described by Cramer et al. (2004) with the following modifications: (1) a small "door" is made in the egg, 1 cm diameter or less to promote long term survival; (2) coelectroporation of several plasmids together requires a high plasmid concentration, 5.5–7.5 μg/μl in sterile dH2O; (3) 5–10 pulse trains at 25–35 V, 50 ms, 10 pulses each with the negative electrode in the center of the neural tube and the positive electrode lateral to rhombomeres 5/6 (r5/r6). Doxycycline (Dox; 1 mg/ml) (Sigma) in sterile buffer (0.1 mg/ml in HANKS:140 mM NaCl, 5.4 mM KCl, 5.6 mM glucose, 0.34 mM Na_2HPO_4, 10 mM HEPES, 1 mM MgCl2, 1 mM CaCl2 pH 7.0) (Sato et al., 2007) was added by pipetting 50 μl of drug onto the chorioallantoic membrane at the times indicated in each experiment.

Tissue preparation, immunostaining, and imaging. Brains were dissected out of the embryo, fixed overnight in 4% PFA and rinsed in PBS. The brainstem was removed and either frozen in OCT blocks for coronal cryosections (12 μm), or embedded in 3% agarose/PBS for coronal vibratome sections (70 μm). Primary antisera diluted in 5% NGS/0.3% Triton X-100/PBS (TrkB, 1:4000, from F. Lefcort) (MAP2, 1:1000, Millipore Bioscience Research Reagents) was added at 4° for 24–72 h. Sections were rinsed 3–4× with PBS, incubated with the appropriate AlexaFlour secondary (1:2000, Invitrogen) for 1–2 h room temp, rinsed three times with PBS, and mounted in Fluoromount-G (Southern Biotechnology). Slides were imaged with an Olympus Fluoview FV1000 confocal microscope with a 10×, 20×, or 60× (NA 1.4; oil) objective.

Slice preparation for electrophysiology. Acute brainstem slices were prepared from electroporated chick embryos at E16 and E18 as described previously (Sanchez et al., 2010). Briefly, the brainstem was dissected and isolated in ice-cold (~0°C) oxygenated low-Ca^{2+} high-Mg^{2+} modified artificial CSF (ACSF) containing the following (in mM): 130 NaCl, 3 KCl, 1.25 NaH_2PO_4, 26 $NaHCO_3$, 4 $MgCl_2$, 1 $CaCl_2$, and 10 glucose. ACSF was continuously bubbled with a mixture of 95% O_2/5% CO_2 (pH 7.4, osmolarity 295–310 mOsm/L). The brainstem was blocked coronally, affixed to the stage of a vibratome slicing chamber (Technical Products International), and submerged in ice-cold ACSF. Bilaterally symmetrical coronal slices were made (200–300 μm thick) and approximately three to six slices (depending on age) containing NM and NL were taken from caudal to rostral, approximately representing the low- to high-frequency regions of NM and NL, respectively.

Slices were collected in a holding chamber and allowed to equilibrate for 1 h at 36°C in normal ACSF containing the following (in mM): 130 NaCl, 3 KCl, 1.25 NaH_2PO_4, 26 $NaHCO_3$, 1 $MgCl_2$, 3 $CaCl_2$, and 10 mM glucose. Normal ACSF was continuously bubbled with a mixture of 95% O_2/5% CO_2 (pH 7.4, osmolarity 295–310 mOsm/L). Slices were allowed to cool to room temperature for 30 min before being transferred from the holding chamber to a 0.5 ml recording chamber mounted on an Olympus BX51W1 microscope for electrophysiological experiments. The microscope was equipped with a CCD camera, 60× water-immersion objective, and infrared differential interference contrast optics. The recording chamber was superfused continuously at near physiologic temperatures (monitored at ~33°-35°C) in oxygenated normal ACSF at a rate of 1.5–2 ml/min.

Whole-cell electrophysiology. Current-clamp experiments were performed using an Axon Multiclamp 700B amplifier (Molecular Devices). Patch pipettes were pulled to a tip diameter of 1–2 μm and had resistances ranging from 3–6 MΩ. The internal recording solution contained the following (in mM): 105 K-gluconate, 35 KCl, 1$MgCl_2$, 10 HEPES-K^+, 5 EGTA, 4ATP-Mg^{2+}, and 0.3 GTP-Na^+, pH adjusted to 7.3 with KOH. The liquid junction potential was 10 mV and data were adjusted accordingly.

A small hyperpolarizing (−1 mV, 100 ms) voltage command was presented at the beginning of each recorded trace to document and monitor whole-cell parameters [resting membrane potential (RMP), cell membrane capacitance, series resistance, and input resistance]. RMPs were measured immediately after break-in. Neurons were included in the data analysis only if they had series resistances <15 MΩ. Raw data were low-pass filtered at 2 kHz and digitized at 20 kHz using a Digidata 1440A (Molecular Devices).

Pipettes were visually guided to NM and neurons were identified and distinguished from surrounding tissue based on cell morphology and location of the nucleus within the slice. All experiments were conducted in the presence of a $GABA_A$-R antagonist picrotoxin (PTX, 100 μM), an AMPA-R antagonist 1,2,3,4-tetrahydro-6-nitro-2,3-dioxo-benzo[*f*]quinoxaline-7-sulfonamide disodium salt hydrate (NBQX, 20 μM) and a NMDA-R antagonist DL-2-amino-5-phosphonopentanoic acid (DL-APV, 100 μM). After a GΩ seal was attained, membrane patches were ruptured and NM neurons were held in whole-cell configuration at $I = 0$ for recording of intrinsic properties. Somatic current injections ranged from −500 to +500 pA, steps of 5–10 mV, and duration lengths of 200–300 ms.

Data analysis and reagents. Recording protocols were written and run using Clampex acquisition and Clampfit analysis software (version 10.1; Molecular Devices). Statistical analyses and graphing protocols were performed using Prism (GraphPad versions 5.0a). All bath applied drugs were allowed to perfuse through the recording chamber for ~2 min before recordings were obtained. DL-APV, NBQX, and all other salts and chemicals were obtained from Sigma-Aldrich. PTX was obtained from Tocris Bioscience.

Results

Focal electroporation and stable expression of *Tol2* plasmids in chick embryos

Tol2-mediated gene transfer was used previously to obtain stable expression of EGFP in chick retinal neurons (Sato et al., 2007). To establish whether a similar approach could be used to achieve gene expression in NM and NL neurons of chick hindbrain auditory circuits, pCAGGS-mbEGFP, a plasmid containing the constitutively active CAGGS promoter regulating expression of membrane associated EGFP, was electroporated into E2 chick

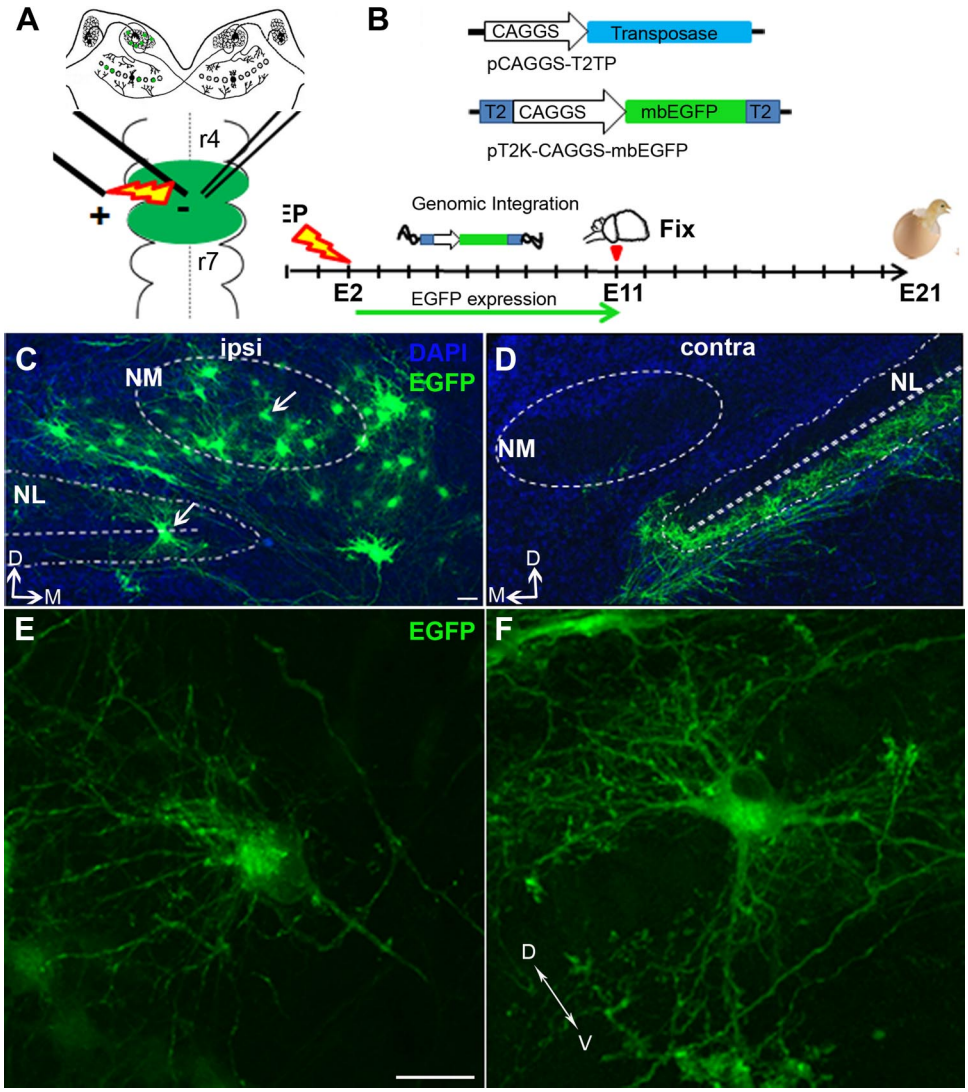

Figure 1. *Tol2*-mediated gene transfer of mb-EGFP by *in ovo* electroporation at rhombomeres 5 and 6 results in stable expression in NM and NL. ***A***, Schematic of DNA injection (green) into the neural tube and placement of electrodes. Current pulses direct DNA to one side of the embryo. Above is representation of a coronal section through auditory brainstem at E11 depicting the result-EGFP expression in cells in NM and NL on one side of the brain. ***B***, *Tol2*-flanked sequences CAGGS-mbEGFP are stably incorporated into the genome and EGFP expression is apparent when the brain is fixed at E11. ***C***, EGFP expression in NM and a few NL cells at E11 on the electroporated side of the embryo (ipsi). Dashed lines are around NM and NL and through the layer of cell bodies of NL. Arrows point to cells depicted at higher magnification in ***E*** (NM) and ***F*** (NL). ***D***, NM and NL on side of brainstem contralateral to electroporation. EGFP completely fills NM axons crossing the midline. ***E***, ***F***, High magnification of cells in ***C***, deconvolved with Huygens software. Scale bars: (in ***C***) ***C***, ***D***, 50 μm; (in ***E***) ***E***, ***F***, 10 μm. D, Dorsal; M, medial; V, ventral.

neural tube along with a plasmid encoding the *Tol2* transposase. Transient expression of the transposase promotes stable chromosomal integration of CAGGS-mbEGFP. Based on fate map data (Cramer et al., 2000), NM and NL neurons were targeted by focal electroporation of the two plasmids into the left side of the neural tube, at r5 and r6 of HH stage 12 embryos. Confocal immunofluorescence microscopy demonstrated expression of EGFP in NM and NL neurons 9 d later (E11). EGFP was distributed throughout the cell soma, in axons of NM neurons in both ipsilateral and contralateral projections, and in the dendrites of NL neurons (Fig. 1*C–F*). Although transfection efficiency varied among embryos, the electroporation parameters used here typically resulted in 5–10% of NM neurons expressing EGFP, while the efficiency of expression of EGFP in NL neurons was typically <5%. EGFP expression also was observed in some cells surrounding NM and NL (Fig. 1*C*), which had morphologies characteristic of both neurons and glia previously observed with Golgi staining (Jhaveri and Morest, 1982c).

Doxycyline regulation of an EGFP reporter

In studies examining events that occur late in development, constitutive overexpression of genes of interest is problematic; because effects of expression during the early stages of development may confound interpretation of changes seen later in development. Consequently, it is essential for our studies to be able to control the timing of transposon-mediated gene expression. For this purpose, we adopted a tet-on system (Gossen et al., 1995), as adapted to the *Tol2* system (Sato et al., 2007). These investigators generated the *Tol2*-derived plasmid, pT2K-BI-TRE-EGFP, which contains a bidirectional tet-on promoter (TRE)-driving expression of the EGFP reporter and a second gene of interest from opposite DNA strands. They also generated the plasmid, pT2K-CAGGS-rtTA-M2, which constitutively expresses a Dox-binding protein (Urlinger et al., 2000, Sato et al., 2007). They demonstrated that coelectroporation of these two plasmids, along with the plasmid-generating transient transfection of the *Tol2* transposase, caused Dox-dependent expression of EGFP in somatic

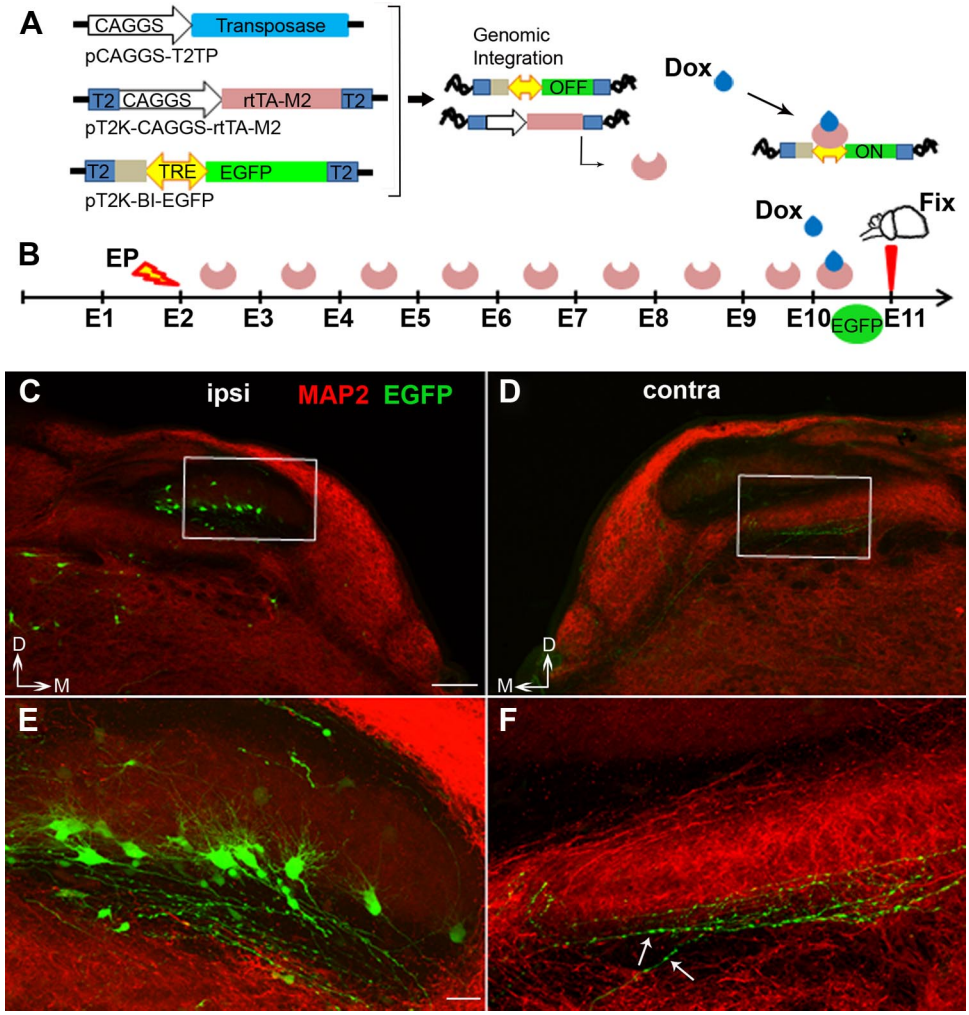

Figure 2. Expression of an EGFP reporter is inducible with Dox at E11. ***A***, Plasmids coelectroporated at E2, transposase, pCAGGS-T2TP, Dox-binding protein pT2K-CAGGS-rtTA-M2, and EGFP reporter pT2K-BI-TRE-EGFP in a 1:1:1 ratio at a total plasmid DNA concentration of 6–6.5 μg/μl. ***B***, Dox-binding protein is constitutively expressed, but not active until Dox is added, and then the complex binds to and activates transcription of EGFP. ***C***, Dox-induced expression of EGFP on one side of the brainstem (ipsi) after 24 h Dox addition (50 μg) to chorioallantoic membrane. ***D***, EGFP-filled fibers of contralateral NM axons synapsing in the ventral neuropil of NL. ***E***, Higher magnification of boxed region in ***C*** shows the cytoplasmic EGFP brightly labels NM axons synapsing on the dorsal, ipsilateral NL dendrites, and in ***F***, a higher magnification of boxed region in ***D*** showing contralateral connections on the ventral dendrites of NL. Arrows point out a few of the many bead-like varicosities on the NM axons. Scale bars: (in ***C***) ***C***, ***D***, 100 μm; (in ***E***) ***E***, ***F***, 20 μm. D, Dorsal; M, medial.

cells until at least E8. For our purposes, it was necessary to demonstrate that this system could achieve Dox-dependent gene expression in neurons, and that the expression could be maintained at developmental ages past E11. The three plasmids were electroporated unilaterally into r5 and r6 of the neural tube at HH stage 12, and Dox (50 μg in 50 μl) was pipetted onto the chorioallantoic membrane at E10. Expression of EGFP was observed throughout NM cells on one side of the brain at E11 (Fig. 2*C*,*D*). MAP2 immunostaining was used to demarcate the dendrites of NL cells, the target of EGFP-expressing NM axons (Fig. 2*E*,*F*). The reporter here is a cytoplasmic EGFP protein that fills the axons of NM neurons completely, allowing details of axon morphology such as their bead-like appearance (Jhaveri and Morest, 1982b) to be clearly visible, even as far as the contralateral terminals in the ventral NL neuropil, 50–80 μm from the NM soma.

EGFP-labeled cells develop normal morphology and physiology

We performed extensive studies to verify that the transposons and their encoded gene products EGFP and Dox-binding protein did not have nonspecific effects on neuronal development, and we could not detect any deleterious effects. Imaging EGFP-expressing NM cells at higher magnification (Fig. 3*A*,*D*) showed that the cells appear similar morphologically to those described previously using the Golgi staining method (Jhaveri and Morest, 1982b) and HRP labeling methods (Young and Rubel, 1986). At E11 all NM cells possess extensive dendritic arbors and a single axon that bifurcates into an ipsilateral and a contralateral projection. All EGFP-expressing NM cells imaged at E10 and E11 resembled those shown in Figure 3*C*. By E16, >95% of rostral NM cells had a spherical soma and had retracted their dendrites, some of which remained as small stubs, typically 1–2 μms in length. (Fig. 3*D*,*F*). In most embryos, 5–10% of NM cells expressed Dox-induced EGFP at E11 and at E16–E18.

To verify that transposon-mediated gene expression does not have nonspecific effects on biophysical properties of neurons, we compared the properties of EGFP-expressing neurons and neighboring neurons that did not express EGFP. Current-clamp studies were performed on NM neurons at E16 using hyperpolarizing and depolarizing somatic current injections (Fig. 4). NM neurons at this age have been shown to exhibit a single action potential and low input resistance (Reyes et al., 1994, Rathouz and Trussell,

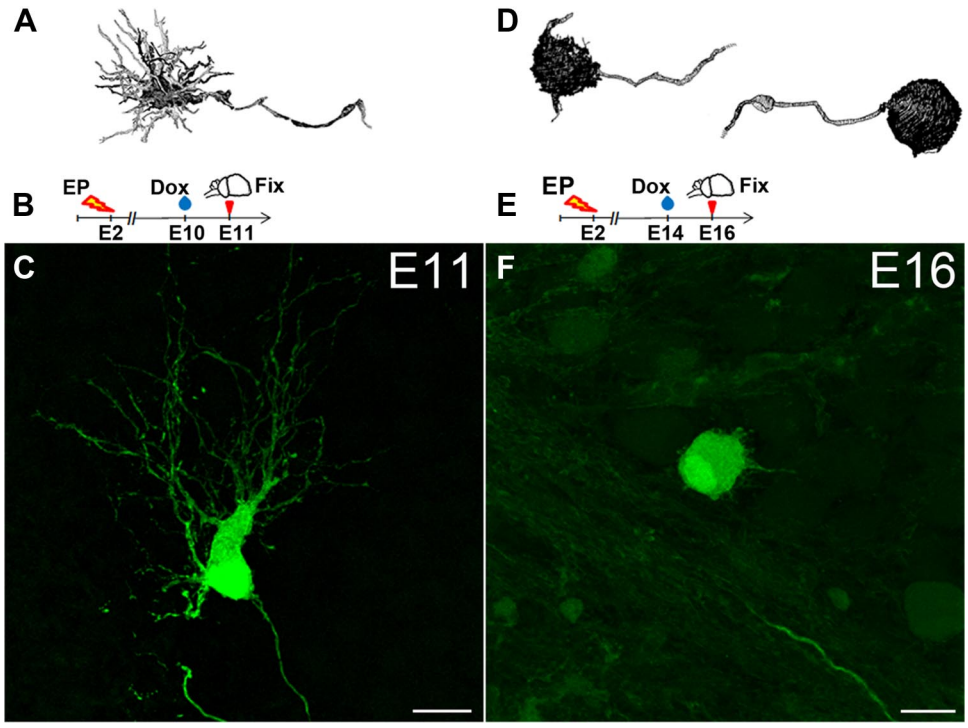

Figure 3. EGFP-expressing cells in NM develop normal morphology. ***A***, ***D***, Golgi-stained cells, at E11 (***A***) and E16 (***D***), images reprinted from Jhaveri and Morest (1982b) with permission from Elsevier. ***B***, ***E***, Summary of time courses of experiments corresponding to cell images shown in ***C*** and ***F***, respectively. ***C***, EGFP expressed in NM neuron at E11 following Dox exposure at E10. ***F***, EGFP expressed in NM neuron at E16 following Dox exposure at E14. Scale bars, 10 μm.

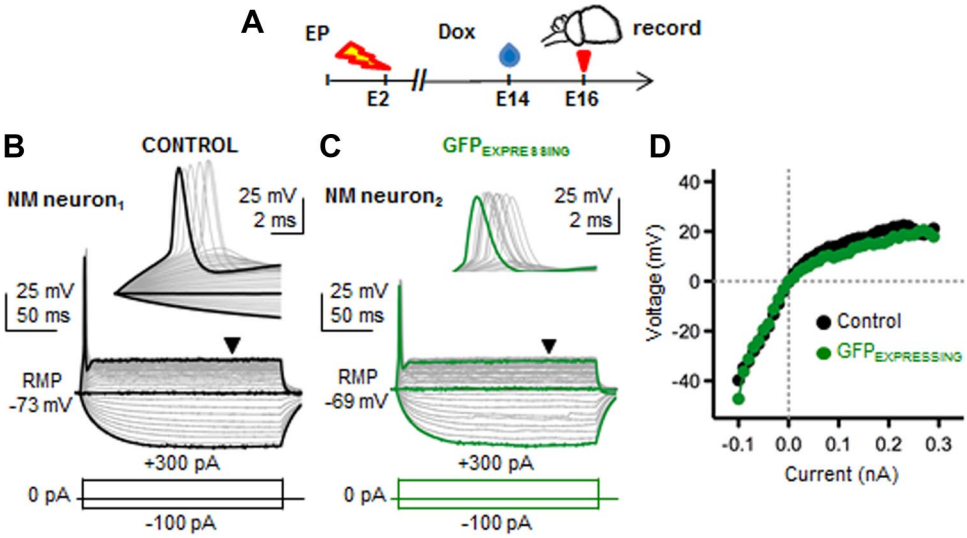

Figure 4. Comparable responses between nontransfected and transfected NM neurons to somatic current injections. Paired current-clamp recordings were performed with E16 NM neurons. EGFP-only plasmid was electroporated at E2 and Dox-treatment was applied at E14. ***A***, Time course of the experiment. ***B***, ***C***, Representative traces from nontransfected (CONTROL; ***B***) and adjacent transfected ($EGFP_{EXPRESSING}$; ***C***) NM neurons. Insets in ***B*** and ***C*** show changes in membrane voltage and action potential generation during the first 16 ms of the response. Calibration: 25 mV, 2 ms. Somatic current injections = −100 to +300 pA, steps 10 pA. ***D***, Voltage-current curves constructed from the 150 ms time point (arrowhead in ***B*** and ***C***) showing overlapping responses to somatic current injections.

1998, Howard et al., 2007). Both EGFP-expressing neurons and non-EGFP-expressing neurons fired a single action potential with similar characteristics (Fig. 4*B*,*C*). Voltage-current (*V*–*I*) curves showed delay inward rectification and low input resistance (Fig. 4*D*), a result consistent with previous reports of age-matched chicken NM neurons (Howard et al., 2007). This result is indicative of biophysical properties highly dependent on voltage-dependent potassium conductances as previously described for NM neurons (for review see, Burger and Rubel, 2008), and demonstrates that expression of EGFP does not influence physiological features.

Doxycycline regulation of EGFP and RFP in a bicistronic transposon

It is experimentally advantageous to be able to express EGFP and a second gene of interest from the same transposon. Use of a

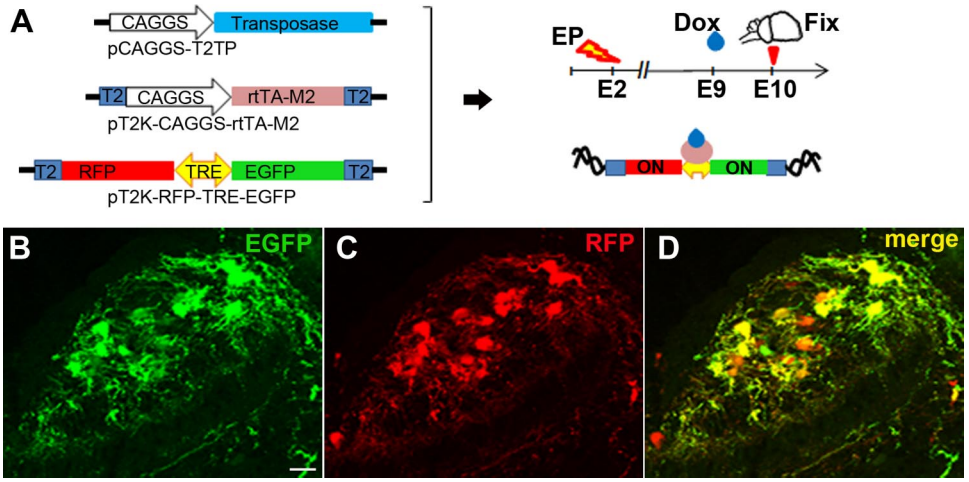

Figure 5. Dox-induced coexpression of a gene of interest, RFP and the EGFP reporter. ***A***, RFP was cloned into pT2K-BI-TRE-EGFP, the three plasmids were coelectroporated at E2 at a concentration of 6–6.5 μg/μl in a 1:1:1 ratio. Dox was added for 24 h at E9. ***B***, ***C***, ***D***, NM-expressing EGFP and RFP. Scale bar (in ***B***) ***B***, ***C***, ***D***: 20 μm.

single promoter-driving expression of EGFP and a second gene from opposite DNA strands of *Tol2* transposons has been reported for several genes (Watanabe et al., 2007). However, these experiments were ended <48 h post-electroporation and no direct verification of expression of genes of interest was provided. To determine the efficiency of the bidirectional promoter, RFP was inserted opposite from EGFP. Chick embryos were electroporated as before, and expression of EGFP and RFP was examined 24 h after addition of Dox at E10. Figure 5*B–D* demonstrate that the bicistronic vector functioned in neurons as intended at a mid-embryonic age. The fraction of NM neurons expressing EGFP and RFP in electroporated embryos was in the range of 5–10%. Both EGFP and RFP were expressed, and their expression was highly correlated. Neurons that expressed EGFP also expressed RFP and vice versa, although the levels of each protein varied among neurons, as observed by their fluorescence. Every neuron expressing EGFP expressed some level of RFP, and only two RFP-expressing neurons were observed to express no EGFP florescence above background.

Doxycycline regulation of TrkB

Having demonstrated that the vector system functions as intended, we adapted the vector to allow manipulation of TrkB expression, replacing RFP in the bicistronic vector with a sequence encoding chicken TrkB, creating the plasmid pT2K-TrkB-BI-TRE-EGFP. TrkB mRNA and protein normally becomes undetectable in NM neurons after E8, 2–3 d before dendrite retraction, suggesting the hypothesis that cessation of TrkB expression is necessary for dendrite retraction. To test this hypothesis, we used the TrkB transposon to artificially maintain TrkB expression in NM past E8. Embryos were electroporated at E2 with plasmids encoding transposase, transposon vector-encoding Dox-binding protein, and transposon vector-encoding EGFP and TrkB (or encoding EGFP alone in controls). Dox application was begun at E7.5, and was repeated every other day through E16.

In the control embryos expressing EGFP but not TrkB, EGFP-expressing NMs had the dendritic branching pattern expected for their location along the rostral–caudal axis of the nucleus. Most NM neurons were adendritic, while the caudal-most NM neurons retained their dendrites (Fig. 6*B*,*C*). A dendrite was defined as a process separate from the axon with a length >5 μms, and a neuron was described as having dendritic morphology if two or more processes longer than 5 μms extended from the soma. In NM from three animals imaged at E17, 70 out of 72 EGFP-expressing rostral NM neurons did not possess dendrites, based on our criteria. However, neurons expressing TrkB with EGFP possessed dendrites at E17, regardless of their rostral–caudal position in NM (Fig. 6*E–H*). We observed 25 TrkB-expressing neurons with dendritic morphology in nine animals, E16–E18, in the rostral region of NM, and no neurons expressing TrkB that did not have dendritic morphology. Immunohistochemical visualization of TrkB revealed that expression levels of TrkB protein in transfected NM neurons were not extremely elevated, but appeared similar to endogenous levels of TrkB in neurons elsewhere in the chick brain, as illustrated for NL neurons (Fig. 6*I*).

To facilitate direct comparison of dendritic structure of TrkB-expressing NM neurons with adjacent neurons that lack TrkB expression, some embryos were electroporated with a mixture of transposon vectors expressing DsRed and transposon vectors expressing TrkB and EGFP. DsRed expression was achieved with a *PiggyBac* (PB) transposable element-based plasmid pPB-loxP-DsRed-loxP-EGFP. Fewer than 5% of NM neurons expressed DsRed in embryos electroporated with this vector, a lower efficiency than observed for the other vectors we have used, possibly reflecting the greater size of this vector's transposon. Expression of fluorescent proteins has been widely used as a means of assessing dendrite morphology (Ivanov et al., 2009). We confirmed that DsRed expression delineated the full dendritic arbors of E11 and caudal E17 NM neurons (data not shown). The pPB-loxP-DsRed-loxP-EGFP transposon expresses DsRed unless cells are exposed to Cre recombinase, in which case the DsRed gene is deleted and EGFP is expressed. Under the conditions of our experiment, the *PiggyBac* transposon expressed DsRed constitutively and did not express EGFP. Rostral NM neurons from two embryos expressing only DsRed (29 neurons total) appeared adendritic at E17, similar to EGFP-expressing and nontransfected rostral NM neurons. Individual neurons potentially may integrate both EGFP/TrkB and DsRed-expressing transposons. However, we observed very few neurons expressing both EGFP and DsRed.

In the absence of Dox administration, no "leaky" expression of EGFP was observed at early stages (E4–E11, data not shown) and no expression of EGFP or TrkB was seen at E17 (Fig. 7*B–E*).

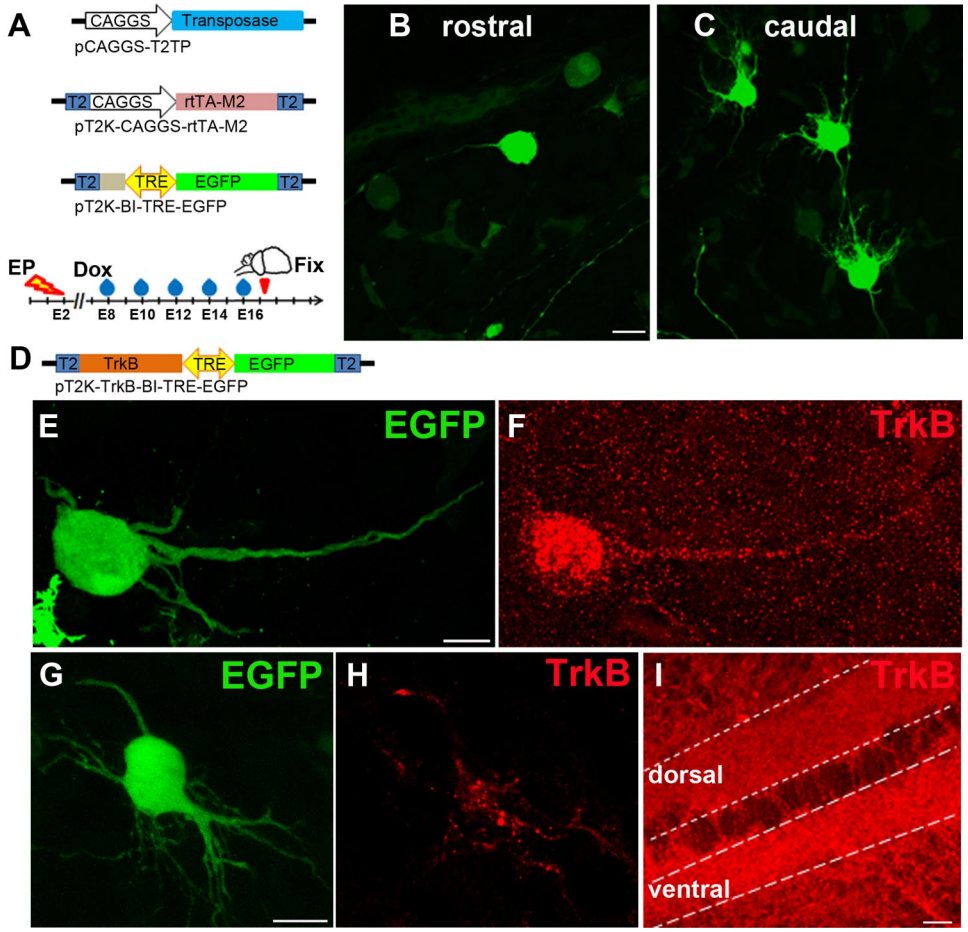

Figure 6. NM neurons for which TrkB expression has been maintained from E8 to E17 have dendrites. ***A***, Embryos were electroporated with *Tol2*-Dox plasmids and treated with Dox from E8–E17. ***B***, ***C***, Images of rostral and caudal regions of NM respectively, at E17. ***D***, TrkB-coding sequences inserted into pT2K-BI-TRE-EGFP. ***E***, ***G***, NM neurons at E17 from two different embryos in which TrkB expression was maintained from E8–E17. ***F***, ***H***, TrkB immunoreactivity in neurons represented in ***E*** and ***G***, respectively. ***I***, TrkB immunostaining of NL ventral dendrites at E12. Area within small dashed lines is the dorsal neuropil, the area within the large dashed lines contains the ventral dendrites (Fig. 1*A*, refer to schematic). At E12, endogenous TrkB is present more abundantly in the ventral dendrites than in the dorsal dendrites and the level of expression is similar to TrkB resulting from Dox-regulated transgene expression in NM, as illustrated in ***F*** and ***H***. Scale bars: (in ***B***, ***G***, ***E***, ***I***) ***B***, ***C***, ***E–I***, 10 μm.

When transposon-encoded TrkB expression was maintained by exposure of embryos to Dox from E7.5–E16, rostral NM neurons expressing DsRed retracted their dendrites normally at E17, exhibiting morphology similar to that observed previously for EGFP-expressing neurons at this age (Figs. 3*F*, 6*B*), whereas adjacent rostral NM neurons expressing TrkB/EGFP retained dendrites (Fig. 7*F–H*). These results support the conclusion that cessation of TrkB expression is necessary for developing NM neurons to retract their dendrites.

We were curious whether the immature appearing dendritic morphology of NM neurons expressing TrkB was accompanied by the maintenance of immature biophysical properties. Current-clamp recordings done at E18 revealed that TrkB-expressing neurons had a much different biophysical profile compared with their wild-type neighboring neurons in the same slice (Fig. 8*A–D*). Responses to hyperpolarizing somatic current injections revealed a lack of time-dependent "voltage-sag" in the NM neuron expressing TrkB (Fig. 8*B*, *C*, arrows). In addition, suprathreshold depolarizing somatic current injections generated multiple action potentials in NM neurons expressing TrkB, while the non-transfected neighboring NM generated only a single action potential (Fig. 8, compare *B*, *C*), a characteristic behavior of mature NM neurons (Reyes et al., 1994). Finally, the generation of one versus multiple APs was also observed at the neuron's threshold for AP initiation (Fig. 8*D*,*E*), suggesting that the expression of TrkB alters developmental changes of biophysical properties of voltage-dependent ion channels, like potassium and I_H conductances, promoting the maintenance of properties typically found in immature NM neurons (Howard et al., 2007).

Discussion

In this report, we introduce use of a *Tol2* transposon-based vector system incorporating a tet-on promoter to obtain stable, focal, and temporally regulated expression of genes of interest in developing chick embryos. We use this system to artificially express the neurotrophin receptor, TrkB, in NM neurons in the chick auditory brainstem. Artificially prolonging the expression of TrkB over the course of embryonic development prevented the normal retraction of dendrites by NM neurons during the late stage of development and altered their biophysical properties. These results support the conclusion that the normal developmental cessation of TrkB expression in NM neurons that occurs ~E8 is necessary for these neurons to attain their normal mature morphology and functional properties. Numerous studies have documented the importance of TrkB signaling for dendritic growth and arborization (McFarlane, 2000). Our study is somewhat un-

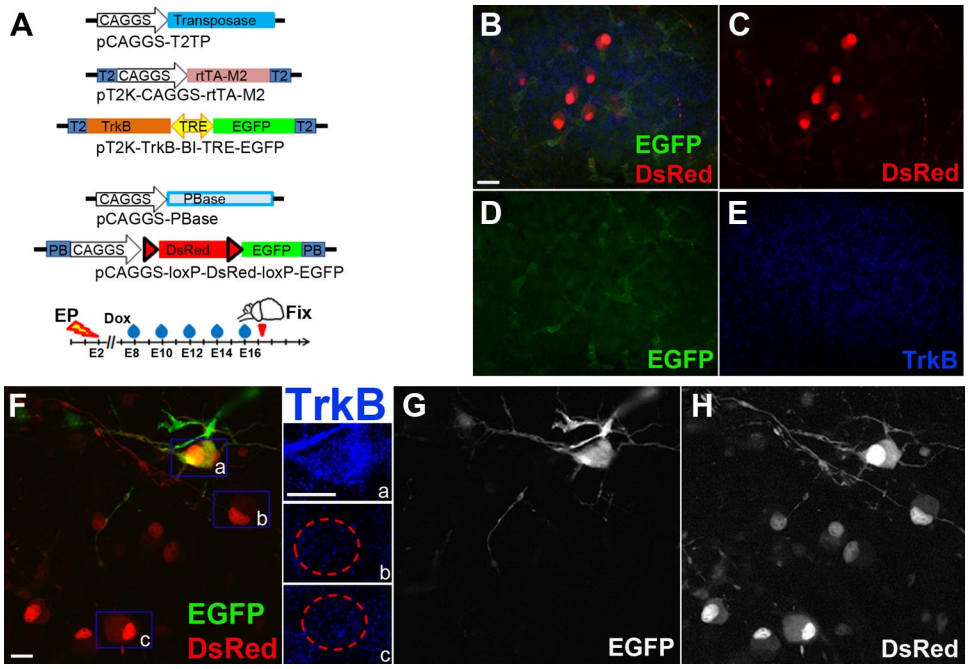

Figure 7. DsRed fluorescent label confirms that NM neurons lacking artificially maintained TrkB expression lack dendrites at E17. ***A***, Transposon-based constructs used to achieve constitutive expression of DsRed and/or Dox-regulated expression of EGFP and TrkB. ***B–E***, In embryos not exposed to Dox, electroporated NM cells at E17 express DsRed but do not express EGFP or TrkB. ***Fa–c***, ***G***, ***H***, In the rostral region of NM in embryos exposed to Dox from E7 to E17, some NM neurons express TrkB and these neurons possess dendrites, while nearby neurons expressing only DsRed do not possess dendrites. DNA: 7 μg/μl; ratio of pCAGGS-PB:pPB-loxP-DsRed-loxP-EGFP:pCAGGS-T2TP:pT2K-CAGGS-rtTA-M2:pT2K-TrkB-BI-TRE-EGFP (1:1.5:1:1:2). Scale bars: (in ***B***) ***B–E*** 20 μm; (in ***F***, ***a***) ***Fa–c***, ***G–I***, 10 μm.

usual in documenting an instance where the cessation of TrkB signaling is a determinant of dendritic morphology. The success of the approach demonstrates that transposon vector systems are likely to have broad applicability for studying circuit formation in the chick embryo CNS.

Temporal regulation of transposable elements in chick

There are several novel aspects to our use of transposon-based vectors. Transposon-mediated genomic integration of transgenes has emerged as an effective method to achieve stable, long-term expression of transgenes for several species, including fish, flies, mouse, and chicken (Lobo et al., 1999, Kawakami and Noda, 2004, Ding et al., 2005, Lu et al., 2009). The use of three transposable element systems have been reported in chick—*mariner* (Sherman et al., 1998), *Tol2* (Sato et al., 2007), and *PiggyBac* (Yamagata and Sanes, 2008, Lu et al., 2009), the latter two incorporating a drug-inducible component allowing temporal regulation. Tamoxifen induction of an ER-Cre fusion protein achieved induced expression of transgenes throughout embryonic development, up to E19, whereas Dox-dependent induction was demonstrated only at early time points up to E8, and expression of an EGFP reporter and genes of interest were demonstrated only within 48 h post-electroporation (Watanabe et al., 2007). We show that with continued Dox application to the chorioallantoic membrane, expression of the vector-encoded genes can be induced and maintained at least until E18, and that the vector system expressing only EGFP has no observable effect on the development of the embryo, or on differentiation of neurons in the auditory brainstem nuclei. Our results also show that the use of a bicistronic vector system allows one to mark cells expressing a gene of interest (*TrkB* in the present study) with an easily detected marker gene, *EGFP*. The incorporation of a fluorescent marker protein was essential for our studies since only a small proportion of neurons are genetically modified by the transposons. The chimeric expression of genes achieved by these vectors is advantageous, since surrounding cells that have not incorporated the transposon serve as negative controls, revealing whether the effects of expressed genes are cell autonomous.

NM and NL are excellent model systems for study of regulation of dendritic arbors

NM and NL manifest two extremes of dendritic organization paramount to their function in the auditory circuit. NM neurons have extensive dendritic arbors that retract over development as the neurons mature, in a manner that is suitable for the physiologically advantageous formation of somatic synaptic contacts (Jhaveri and Morest, 1982a,b), whereas NL neurons develop complex dorsal and ventral dendritic arbors that vary in length depending on tonotopic position, the dendrites in the low-frequency region being tenfold longer than the dendrites of the high-frequency neurons (Smith and Rubel, 1979). In the present study we have focused on mechanisms controlling the dendritogenesis of NM neurons, but the methods we have described will also be applicable to studying dendritogenesis in NL neurons.

TrkB function in NM neurons

NM neurons normally withdraw their transient dendritic arbor after TrkB expression ceases in these neurons. Our results indicate that the cessation of TrkB expression is necessary for their normal developmental maturation, since artificially prolonging TrkB expression prevents the normal retraction of dendrites. Importantly, the intensity of immunostaining indicates that the vector used achieves artificially encoded TrkB expression in NM at levels that are similar to those that are expressed naturally in developing chick neurons. The ability of TrkB expression to influence the morphology and physiological function of NM neu-

rons implies that TrkB becomes activated in these neurons. We have not yet identified the mode of activation. TrkB activates spontaneously when expressed at excessively high levels (Schecterson and Bothwell, 2010), but the levels of transposon-encoded TrkB expression obtained in the present study do not exceed levels at which TrkB is normally expressed in other neurons. TrkB is commonly activated by BDNF (avians lack the alternative ligand NT-4), although NT-3 can activate TrkB less potently. However, several unpublished studies have failed to detect BDNF or NT3 mRNA in developing avian hindbrain in the vicinity of NM (E. Rubel, personal communication). Elsewhere in the developing nervous system, BDNF is delivered from distant neurons via anterograde axonal transport (von Bartheld et al., 1996, Altar and DiStefano, 1998). Rat spiral ganglion neurons express BDNF (Zha et al., 2001). If avian cochlear ganglion neurons do likewise, their axon terminals may provide BDNF to NM. Alternatively, transactivating effects of certain G-protein coupled receptors (for review, see Schecterson and Bothwell, 2010) may be responsible for TrkB activity in NM. We are engaged in studies to discriminate among these possibilities.

The calycal structure of the endbulbs of Held, the synapses of VIIIth nerve terminals on NM, is highly conserved in homologous circuits from reptiles to mammals, and is thought to be important for maintaining the temporal fidelity of neural activity required for estimating interaural time difference (ITD) (Parks, 1981). The mechanism responsible for specifying the formation of calycal synaptic contacts is entirely unknown. The observation that cochlear ganglion axon terminals on NM neurons transiently form dendritic synaptic contacts, and then convert to calycal somatic synaptic contacts as dendrites are withdrawn, suggests that the elimination of dendrites may be one of the signals that specifies the formation of calycal synaptic contacts. Thus, in NM neurons in which dendrite retraction is prevented by artificially prolonged TrkB expression, one might imagine that dendritic synaptic contacts are maintained, and calycal nerve endings may fail to form. Future studies will address this important question.

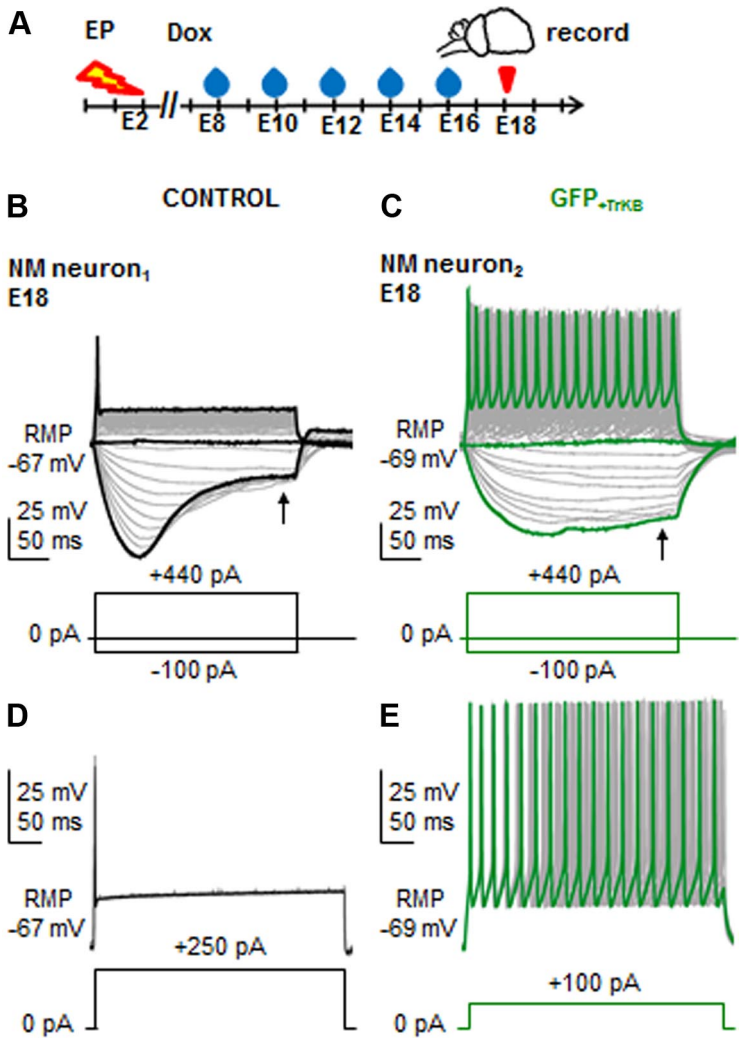

Figure 8. NM neurons expressing or not expressing TrkB respond differently to somatic current injection. ***A***, Time course of the experiment. TrkB plasmid was electroporated at E2 and Dox applied from E7.5 to E16. ***B***, ***C***, Representative paired current-clamp recordings from E18 NM neurons showing responses to somatic current injections from nontransfected (***B***, CONTROL) and adjacent TrkB transfected (***C***, GFP_{+TrkB}) NM neurons. Schematic lines under traces: somatic current injections (−100 to +440 pA, steps 10 pA, 200 ms), minimized for clarity. Black arrows in ***B*** and ***C*** show lack of "voltage-sag" in the transfected NM neuron. ***D***, ***E***, Current-clamp responses to somatic current injection for the same neurons in ***B*** and ***C*** presented at each neuron's threshold for AP initiation (***D***, +250 pA, CONTROL neuron, schematic line under trace, 500 ms; ***E***, +100 pA, GFP_{+TrkB} neuron, schematic line under trace, 500 ms; minimum of 15 overlapping traces for each neuron).

Although we have not yet determined whether the nature of synaptic contacts on NM neurons is altered by prolonged TrkB expression, we have demonstrated that the electrophysiological properties of NM neurons are substantially different from those normally seen at this age and similar to those seen in much younger embryos. Current-clamp recordings were performed on TrkB-expressing neurons marked by coexpressed EGFP and on neighboring, TrkB-negative neurons in the same animal as controls. These recordings showed that the E18 TrkB-expressing neurons are similar in overall behavior to much younger MN neurons in many respects and much different from normal E18 NM neurons or neighboring NM neurons not expressing TrkB.

In mature NM neurons, the characteristic firing of a single action potential is highly regulated by low- and high-voltage dependent potassium channels (Reyes et al., 1994, Parameshwaran et al., 2001, Lu et al., 2004). By E14, nearly all NM neurons have acquired this characteristic firing property and by E18 all NM neurons act similarly in this respect (Howard et al., 2007). At E10, however, NM neurons do not maintain clamped membrane potentials during strong depolarizing current steps, thereby usually firing multiple APs to a sustained depolarization. In addition, younger NM neurons have broader APs and the AP threshold is lower than found in older neurons. In our studies, TrkB-expressing neurons reliably showed these younger phenotypes, with multiple spikes, broader action potentials, and lower thresholds than their neighboring neurons that were not expressing TrkB.

However, in some ways the TrkB-expressing neurons displayed biophysical features unlike either normal E10 or E18 NM

neurons. At E10, APs in normal NM neurons occur only at the beginning of a prolonged depolarizing current step and never in the later segment. Surprisingly, TrkB-expressing neurons reliably generated APs throughout the entire duration of prolonged depolarizing current steps. The ability of the TrkB-positive neurons to fire continuous action potentials to sustained somatic current injections may be due to alterations in potassium channels expression and function. It remains to be determined whether this reflects a direct effect of TrkB on channel expression or function, or alternatively, whether these channels are influenced by altered synaptic transmission resulting from TrkB-mediated maintenance of dendritic arbors.

In conclusion, we have combined the use of transposon-mediated transgene expression and focal *in ovo* electroporation to temporally manipulate gene expression in specific auditory nuclei in the chick brainstem, providing novel insights into the function of TrkB in dendritic regulation. The chick embryo has been one of the most widely used systems for study of vertebrate development for over two centuries (Stern, 2005). The novel methods applied here can easily be adapted to characterize the function of other genes and in other CNS neural circuits.

References

Altar CA, DiStefano PS (1998) Neurotrophin trafficking by anterograde transport. Trends Neurosci 21:433–437. CrossRef Medline

Burger RM, Rubel EW (2008) Encoding of interaural timing for binaural hearing In: The senses: a comprehensive reference (Dallos P, Oertel D, eds), pp 613–30. San Diego: Academic.

Cochran SL, Stone JS, Bermingham-McDonogh O, Akers SR, Lefcort F, Rubel EW (1999) Ontogenetic expression of trk neurotrophin receptors in the chick auditory system. J Comp Neurol 413:271–288. CrossRef Medline

Cramer KS, Fraser SE, Rubel EW (2000) Embryonic origins of auditory brain-stem nuclei in the chick hindbrain. Dev Biol 224:138–151. CrossRef Medline

Cramer KS, Bermingham-McDonogh O, Krull CE, Rubel EW (2004) EphA4 signaling promotes axon segregation in the developing auditory system. Dev Biol 269:26–35. CrossRef Medline

Ding S, Wu X, Li G, Han M, Zhuang Y, Xu T (2005) Efficient transposition of the piggyBac (PB) transposon in mammalian cells and mice. Cell 122: 473–483. CrossRef Medline

Gossen M, Freundlieb S, Bender G, Müller G, Hillen W, Bujard H (1995) Transcriptional activation by tetracyclines in mammalian cells. Science 268:1766–1769. CrossRef Medline

Howard MA, Burger RM, Rubel EW (2007) A developmental switch to GABAergic inhibition dependent on increases in Kv1-type K+ currents. J Neurosci 27:2112–2123. CrossRef Medline

Ivanov A, Esclapez M, Pellegrino C, Shirao T, Ferhat L (2009) Drebrin A regulates dendritic spine plasticity and synaptic function in mature cultured hippocampal neurons. J cell science 122:524–534. CrossRef Medline

Jhaveri S, Morest DK (1982a) Sequential alterations of neuronal architecture in nucleus magnocellularis of the developing chicken: an electron microscope study. Neuroscience 7:855–870. CrossRef Medline

Jhaveri S, Morest DK (1982b) Sequential alterations of neuronal architecture in nucleus magnocellularis of the developing chicken: a Golgi study. Neuroscience 7:837–853. CrossRef Medline

Jhaveri S, Morest DK (1982c) Neuronal architecture in nucleus magnocellularis of the chicken auditory system with observations on nucleus laminaris: a light and electron microscope study. Neuroscience 7:809–836. CrossRef Medline

Kawakami K, Noda T (2004) Transposition of the Tol2 element, an Ac-like element from the Japanese medaka fish *Oryzias latipes*, in mouse embryonic stem cells. Genetics 166:895–899. CrossRef Medline

Lobo N, Li X, Fraser MJ (1999) Transposition of the piggyBac element in embryos of *Drosophila* melanogaster, *Aedes aegypti* and *Trichoplusia ni*. Mol Gen Genet 261:803–810. CrossRef Medline

Lu Y, Monsivais P, Tempel BL, Rubel EW (2004) Activity-dependent regulation of the potassium channel subunits Kv1.1 and Kv3.1. J Comp Neurol 470:93–106. CrossRef Medline

Lu Y, Lin C, Wang X (2009) PiggyBac transgenic strategies in the developing chicken spinal cord. Nucleic Acids Res 37:e141. CrossRef Medline

Luikart BW, Nef S, Virmani T, Lush ME, Liu Y, Kavalali ET, Parada LF (2005) TrkB has a cell-autonomous role in the establishment of hippocampal Schaffer collateral synapses. J Neurosci 25:3774–3786. CrossRef Medline

McFarlane S (2000) Dendritic morphogenesis: building an arbor. Mol Neurobiol 22:1–9. CrossRef Medline

Parameshwaran S, Carr CE, Perney TM (2001) Expression of the Kv3.1 potassium channel in the avian auditory brainstem. J Neurosci 21:485–494. Medline

Parks TN (1981) Morphology of axosomatic endings in an avian cochlear nucleus: nucleus magnocellularis of the chicken. J Comp Neurol 203:425–440. CrossRef Medline

Rathouz M, Trussell L (1998) Characterization of outward currents in neurons of the avian nucleus magnocellularis. J Neurophysiol 80:2824–2835. Medline

Reyes AD, Rubel EW, Spain WJ (1994) Membrane properties underlying the firing of neurons in the avian cochlear nucleus. J Neurosci 14:5352–5364. Medline

Rubel EW, Fritzsch B (2002) Auditory system development: primary auditory neurons and their targets. Annu Rev Neurosci 25:51–101. CrossRef Medline

Rubel EW, Parks TN (1988) Organization and development of the avian brain-stem auditory system. In: Auditory function: neurobiological bases for hearing (Edelman GM, Gall WE, Cowan GM, eds), pp 3–92. New York: Wiley Interscience.

Sanchez JT, Wang Y, Rubel EW, Barria A (2010) Development of glutamatergic synaptic transmission in binaural auditory neurons. J Neurophysiol 104:1774–1789. CrossRef Medline

Sato Y, Kasai T, Nakagawa S, Tanabe K, Watanabe T, Kawakami K, Takahashi Y (2007) Stable integration and conditional expression of electroporated transgenes in chicken embryos. Dev Biol 305:616–624. CrossRef Medline

Schecterson LC, Bothwell M (2010) Neurotrophin receptors: old friends with new partners. Dev Neurobiol 70:332–338. CrossRef Medline

Sherman A, Dawson A, Mather C, Gilhooley H, Li Y, Mitchell R, Finnegan D, Sang H (1998) Transposition of the *Drosophila* element mariner into the chicken germ line. Nat Biotechnol 16:1050–1053. CrossRef Medline

Smith DJ, Rubel EW (1979) Organization and development of brain stem auditory nuclei of the chicken: dendritic gradients in nucleus laminaris. J Comp Neurol 186:213–239. CrossRef Medline

Stern CD (2005) The chick; a great model system becomes even greater. Dev Cell 8:9–17. CrossRef Medline

Urlinger S, Baron U, Thellmann M, Hasan MT, Bujard H, Hillen W (2000) Exploring the sequence space for tetracycline-dependent transcriptional activators: novel mutations yield expanded range and sensitivity. Proc Natl Acad Sci U S A 97:7963–7968. CrossRef Medline

von Bartheld CS, Byers MR, Williams R, Bothwell M (1996) Anterograde transport of neurotrophins and axodendritic transfer in the developing visual system. Nature 379:830–833. CrossRef Medline

Watanabe T, Saito D, Tanabe K, Suetsugu R, Nakaya Y, Nakagawa S, Takahashi Y (2007) Tet-on inducible system combined with in ovo electroporation dissects multiple roles of genes in somitogenesis of chicken embryos. Dev Biol 305:625–636. CrossRef Medline

Xu B, Zang K, Ruff NL, Zhang YA, McConnell SK, Stryker MP, Reichardt LF (2000) Cortical degeneration in the absence of neurotrophin signaling: dendritic retraction and neuronal loss after removal of the receptor TrkB. Neuron 26:233–245. CrossRef Medline

Yacoubian TA, Lo DC (2000) Truncated and full-length TrkB receptors regulate distinct modes of dendritic growth. Nat Neurosci 3:342–349. CrossRef Medline

Yamagata M, Sanes JR (2008) Dscam and Sidekick proteins direct lamina-specific synaptic connections in vertebrate retina. Nature 451:465–469. CrossRef Medline

Young SR, Rubel EW (1986) Embryogenesis of arborization pattern and topography of individual axons in N. laminaris of the chicken brain stem. J Comp Neurol 254:425–459. CrossRef Medline

Zha XM, Bishop JF, Hansen MR, Victoria L, Abbas PJ, Mouradian MM, Green SH (2001) BDNF synthesis in spiral ganglion neurons is constitutive and CREB-dependent. Hear Res 156:53–68. CrossRef Medline